

# TUBING FLOW MODEL FOR PREDICTING BOTTOM HOLE PRESSURE DURING CO<sub>2</sub> INJECTION: CORRELATION OF PRESSURE DATA FROM LARGE-SCALE STORAGE PROJECTS

R.T. Okwen, Illinois State Geological Survey  
J. F. Lea, Production & Lift Technology

## SUMMARY

One requirement of a Class VI Underground Injection Control permit involves continuous monitoring and reporting of injection pressure. Wells in pilot and commercial scale carbon dioxide (CO<sub>2</sub>) storage sites are equipped with devices that measure pressure and flow rate during injection operations. Downhole device failures have occurred during CO<sub>2</sub> injection operations in projects, which prevent bottom hole pressure measurement and require time consuming repairs. A model that can be used to accurately predict bottom hole pressures, based on tubing flow performance, during CO<sub>2</sub> injection is warranted.

This paper uses a two-phase flow model, based on Hagedorn-Brown correlation that uses wellbore parameters and correlated CO<sub>2</sub> properties to predict bottom hole pressures during injection. A finite-difference program that uses CO<sub>2</sub> density and viscosity, wellhead temperature and pressure, bottom hole temperature, tubing diameter, roughness, well length, and injection rate as input to the model was developed for calculating vertical wellbore pressure changes during injection. Input parameters that have some effect on results are presented and discussed.

The program was applied to field injection data from the Illinois Basin Decatur Project and Industrial Carbon Capture and Sequestration projects to evaluate predicting measured bottom hole pressure data. The predictions matched measured bottom hole pressure within □□□□□ (average relative error).

## INTRODUCTION

Carbon dioxide (CO<sub>2</sub>) storage site operators are required to monitor and report bottom hole flowing pressure (BHP) to ensure CO<sub>2</sub> is injected at pressures lower than the parting pressure of storage units, which is a Class VI Underground Injection Control (UIC) permit requirement. Bottom hole flowing pressures can be estimated from corrected surface (wellhead) pressure or measured using installed downhole gauges. Estimating the BHP through wellhead pressure corrections is challenging because CO<sub>2</sub> properties (density, viscosity, and phase) could change as CO<sub>2</sub> traverses from the wellhead to the bottom of the well due to changes in temperature and pressure. Similarly, failure of installed bottom hole gauges could prevent measurement of bottom hole pressures. Time waiting for a rig, killing well, and failed gage retrieval can delay the project days to months. Examples of downhole gauge failures include (1) failure of an electronic component of installed bottom hole pressure gauges including downhole memory gauges, used to replace the pressure gauges, during implementation of a CO<sub>2</sub> injection project at Cranfield, Mississippi, (Hovorka et al. 2013), and (2) intermittent failures of downhole gauges installed in the monitoring well (Locke *et al.* 2018) of the Illinois Basin Decatur Project's (IBDP). As a result, developing capabilities to accurately estimate injection BHP from wellhead pressure or predict measured BHP in the event installed gauges fail is warranted.

The objective of this study is to utilize field injection (pressure, temperature, and rate) data to develop a tool that accurately predict BHP during CO<sub>2</sub> injection. The model will be considered accurate if its predictions closely match measured BHP within □□5% relative error. This will be achieved through application of historical multiphase fluid flow model principles utilized for this application. The proceeding sections of this paper are as follows. Section 2 describes development of a modified Hagedorn-Brown (HB) model for calculating wellbore pressure-depth traverse. In section 3, we describe a workflow for calculating wellbore pressure-depth traverse. Section 4 describes sensitivity of BHP to changes in wellbore parameters

(i.e. step size, pipe roughness, Reynolds number, and friction factor). Section 5 evaluates the uncertainty of the calculated BHP as a function of CO<sub>2</sub> density, wellhead pressure, and depth. In section 6, we applied the modified HB model on field injection data to assess accuracy of the model's predictions. Lastly, sections 7 and 8 discuss application of the modified HB model for wellbore pressure-depth traverse at other CO<sub>2</sub> storage sites and provide conclusions and recommendations for further research.

## BACKGROUND

A well is an interfacing conduit between the surface and the subsurface, used to produce fluids from or inject fluids into a reservoir containing possibly water, oil, or gas in varying percentages. On a high level, a combination of an injection well and the reservoir constitute an injection system. This system consists of components such as a porous medium (reservoir), well completions (perforations, gravel packs), vertical conduit (tubing with packers, chokes and valves), artificial lift system (compressors and pumps) and horizontal flowlines and other piping components (e.g. valves and elbows). In an injection system, fluids flow from the surface, through an injection well, to the reservoir. The bottom hole flowing pressure (BHP), which is dependent on fluid injection rate ( $q_{inj}$ ), fluid properties (density and viscosity), wellhead pressure ( $p_{wh}$ ), tubing roughness, and depth, controls flow of fluids in the injection system. A pressure gradient is established from the wellhead to the reservoir during injection (assuming negligible change in pressure between the compressor and wellhead although this could be calculated if details of pressure delivery line are known).

Any point between the compressor and reservoir boundary, at which pressure can be calculated as a function of flow rate, can be considered as a node. The compressor (1) and reservoir boundary (5) are the extreme nodes of the injection system, i.e., compression ( $p_{comp}$ ) and average reservoir ( $p_r$ ) pressures, respectively (Fig. 1). Nodes at the wellhead (2) bottom hole tubing gauge (3) and bottom hole perforation (4), wellhead pressure ( $p_{wh}$ ), bottom hole tubing pressure (BTP) and (5) BHP are measured or calculated are also important. Pressures at the wellhead and bottom of the tubing are measured using gauges attached to the Christmas tree and downhole. Measured BTP or  $p_{wh}$  (if the reservoir is at the end of the tubing), flow rates and fluid properties can be used to estimate BHP. Because flow rate is functionally related to the pressure change across each component within the injection system, measured pressure can be used to estimate pressure change between nodes as a function of the flow rate.

Understanding the functional relationship between flow rate and pressure loss in the tubing (plumbing system in the well) is vital in estimating BTP and BHP with high degree of accuracy. Depending on the temperature and pressure between the wellhead and bottom of the well, CO<sub>2</sub> may undergo phase change during injection, i.e., it can be a gas, liquid or supercritical fluid. In large-scale storage projects, CO<sub>2</sub> is generally injected at pressures above its critical pressure (1,071 psia) because it is denser and less compressible at high pressure (i.e. to maximize storage). However, CO<sub>2</sub> is not supercritical at the wellhead when temperatures are lower than its critical temperature ( $T_c = 87.8^\circ\text{F}$ ). For example, in the IBDP, compressed and dehydrated CO<sub>2</sub>, from nearby Archer Daniels Midlands (ADM) ethanol processing plant, was inherently heated to temperatures ranging between 80 °F to 102 °F and injected at pressures greater than 1100 psi (1126 psia actually) (Jones and McKaskle, 2014). Without heating, the wellhead temperature will be equivalent to surface temperatures. Surface temperatures are also impacted by location and seasonal changes. Nonetheless, surface temperatures are high (above 70°F), average (below 70°F), and low (below 60°F) in the summer, fall and spring, and winter, respectively. CO<sub>2</sub> is a liquid at the wellhead, where temperatures are lower than  $T_c$ , and transitions into a supercritical fluid while traversing to the well bottom due to increase in temperature with depth. Therefore, a suitable multiphase (two-phase) flow model that accounts for changes in CO<sub>2</sub> density and viscosity is warranted to accurately calculate pressure change along wellbore tubing as function of injection rate.

The tubing performance relationship (TPR) for multiphase fluid flow in pipes is an extension of the TPR of a steady state single-phase incompressible fluid flow, derived from general energy equation (Brown, 1977) The terms that make up the calculated pressure gradient are as follows:

$$144 \frac{dp}{dh} = \frac{g}{g_c} \rho \sin\theta + \frac{f \rho v^2}{2g_c D} + \frac{\rho v dv}{2g_c dh} \quad (1)$$

The pressure change over a length of pipe is found by integrating the pressure gradient along the pipe to calculate the pressure at any given point. The first, second, and third terms on the right-hand side of eq.1 are the hydrostatic (elevation), friction, and acceleration pressure gradients, respectively. The above equation (eq.1) is applicable for any single-phase fluid flow and well inclination. For example, as  $\theta$  approaches zero, the flow type changes from vertical or inclined to horizontal and the hydrostatic term in eq. (1) diminishes. Similarly, the friction and acceleration pressure gradients decline as  $v$  decreases and vice versa. Friction loss is also strongly dependent on inner diameter and friction factor, which is also dependent on Reynolds number and roughness of the conduit e.g. pipes and tubing. It is also applicable to multiphase flow where the phases are uniformly mixed or homogeneous and the density can be calculated.

The multiphase flow TPR is more complicated because of variations in flow regimes or pattern and instability of the interface between fluid phases, all which impact fluid distribution and pressure gradient in conduits, (Hagedorn and Brown 1965, Guo, *et al.* 2007). Bubble, slug, churn, and annular flow regimes have been identified in gas-liquid two-phase flow. As the proportion of gas phase in a continuous liquid phase increases the flow regime progresses from bubble through slug and churn, to annular flow regimes. Gas phase is dispersed as small bubbles in a continuous liquid phase in bubble flow. As the proportion of gas phase increases the bubbles coalesce into larger bubbles, filling the entire cross-section of the pipe and leaving liquid slugs between the bubbles (slug flow). Continual increment in gas phase proportion will lead to instability and collapse of large bubbles, resulting to a highly turbulent flow pattern and both phases dispersed (churn flow). In annular flow, gas becomes a continuous phase and liquid flows on pipe wall. The liquid droplets trapped in the gas phase spread on the pipe wall (Guo, *et al.* 2007).

In a review of TPR models for analyzing multiphase flow in vertical pipes, Brown (1977) classified the models as homogeneous and separated-flow models. In homogeneous models, the multiphase is treated as a homogeneous mixture and assumes negligible slippage (holdup) of the dense phase. Separated-flow models account for effects of slippage and flow regime. Homogeneous flow models are mechanistic and can model three phase and four phase systems. These models are less accurate and generally require calibration to local field conditions. On the other hand, separated-flow models are more realistic and difficult to program compared to homogeneous models because they are modeled using empirical correlations. Because of the complexities involved in multiphase flow modeling, most researchers resorted to using semi- or purely empirical approaches. For example, Hagedorn and Brown (1965) used experimental data from a 1500-ft well to develop correlations for analyzing vertical two-phase flow through tubing of different sizes (1-inch, 1¼-inch, and 1½-inch). Data in the development of the correlations was generated from 475 experiments (Hagedorn, 1964) including additional 106 experiments reported by Fancher and Brown (1963). Pressure gradients, of pipes with diameters greater than 1½-inch, calculated using Hagedorn-Brown correlations closely match experimentally determined values within a degree accuracy enough for engineering calculations (Hagedorn and Brown, 1965). As a result, a modified Hagedorn-Brown (HB) model consisting of the original Hagedorn and Brown (1965) empirical correlation with Griffith correlation (Griffith and Wallis 1961) for bubble flow and no-slip liquid holdup, recommended by Ansari *et al.* (1994) and Hasan and Kabir (2002) was adopted for calculation of pressure traverse (pressure change as a function of depth along the wellbore) during CO<sub>2</sub> injection i.e. homogeneous vertical two-phase flow. Two phase calculations are allowed but the density and viscosity of the CO<sub>2</sub> is brought in from outside sources. As a result, the pressure change is calculated from hydrostatic and friction effects, with hydrostatic being dominant unless high rates are input.

The pressure traverse along a vertical well or conduit ( $\sin \theta = \sin 90^\circ = 1$ ) is calculated using a finite-difference form of equation (1):

$$144 \frac{\Delta p}{\Delta h} = \frac{g}{gc} \rho_m + \frac{f_m \rho_m v_m^2}{2gc d} + \rho_m \frac{\Delta(v_m^2)}{2gc \Delta h} \quad [\text{lb}/\text{ft}^3] \quad (2)$$

If the contribution of the acceleration term (third term on the right-hand-side of eq. 2) is negligible at high flow rates and large tubing diameter (Hagedorn and Brown 1965), simplifies eq. (2) into the following:

$$\Delta p = \frac{\Delta h}{144} \left( \frac{g}{gc} \rho_m + \frac{f_m \rho_m v_m^2}{64.4 d} \right) \quad (3)$$

There are other multiphase flow models, some developed by operators and technical experts, and others developed by companies offering nodal and multiphase flow packages for sale or lease.

### Pressure calculation workflow

A program that uses the modified HB model to calculate downhole pressures (BTP and BHP) as a function of CO<sub>2</sub> properties (density and viscosity), temperature ( $T$ ), wellhead pressure ( $p_{wh}$ ), pipe (tubing) diameter ( $d$ ) and roughness, total well depth ( $D$ ), and injection rate ( $q$ ), was developed. The program uses the depth, pressure, and temperature at the wellhead as initial conditions. It divides the depth into small cells (segments) ( $\Delta h$ ) of size(s) greater than or equal to  $1/50^{\text{th}}$   $D$ , using the wellhead as reference point (Fig. 2). Larger increments can be used up to the point of influencing the final calculated flowing BHP. For instance, it is shown below that 640 ft for the increment size is too large and creates error in the result compared to use of the smaller increments (Table 1 and Fig. 5). Each  $\Delta h$  is considered as a step-in depth from the wellhead to the bottom of the well. The corresponding increment in temperature ( $\Delta T$ ) for each  $\Delta h$  is estimated via linear interpolation of the surface temperature ( $T_{surf}$ ) and bottom hole temperature (BHT) as a function of depth (i.e.  $\Delta T = [BHT - T_{surf}]/\text{Depth}$ ). The depth of each cell ( $h_i$ ) is calculated as the sum of the depth of the preceding cell ( $h_{i-1}$ ) and  $\Delta h$ , i.e.  $h_i = h_{i-1} + \Delta h$ . Using the wellhead pressure ( $p_{i-1} = p_{wh}$ ) as the initial pressure, the pressure at the bottom of the cell ( $p_i$ ) is iteratively calculated as the sum of  $p_{wh}$  and the product of  $\Delta h$  and cell pressure gradient ( $p_{grad}$ ) (i.e.  $p_i = p_{i-1} + p_{grad} \Delta h$ ). The average pressure ( $p_{avg}$ ) at each cell is calculated as the arithmetic mean of  $p_{i-1}$  and  $p_i$ , i.e.,  $p_{avg} = 0.5(p_i - p_{i-1})$ . Similarly, the temperature at the wellhead ( $T_{surf}$ ) is used as the initial temperature ( $T_{i-1}$ ) and temperature at the bottom of the cell ( $T_i$ ) is the sum of  $T_{i-1}$  and the product between  $\Delta T$  and  $h_i$  (i.e.  $T_i = T_{surf} + \Delta T h_i$ ). Average temperature ( $T_{avg}$ ) at each cell is calculated as the arithmetic mean of  $T_{i-1}$  at the top and  $T_i$  at the bottom, (i.e.,  $T_{avg} = \frac{1}{2} [T_i - T_{i-1}]$ ).

In addition, the density and viscosity of CO<sub>2</sub>, which are required for calculating hydrostatic and friction pressure gradients including flow velocity, Reynolds number, and friction factor, are calculated at the  $p_{avg}$  and  $T_{avg}$  of each cell. Data from the National Institute of Standards (NIST) database (Lemmon et al. 2019) were used to develop correlations for calculating CO<sub>2</sub> density and viscosity within 2 - 3% margin of error for temperatures ranging between -50 °F and 200 °F and pressures between 10 psi and 6000 psi. The range of validity of viscosity and density calculated were extended by integrating the correlation developed by Ouyang (2011), which is valid for temperatures and pressures between 104 °F and 212 °F (40 °C and 100 °C) and 1100 psia and 9000 psia (6 and 62 MPa). The superficial flow velocity ( $v_m$ ) is calculated as the ratio of the mass flow rate ( $Q_m$ ) to the product of cross-sectional area of the tubing and CO<sub>2</sub> density at  $p_{avg}$  and  $T_{avg}$  and is calculated using the following equation:

$$v_m = \frac{Q_m}{\rho_m} \left( \frac{\pi d^2}{4} \right)^{-1} \quad (4)$$

The mass flow rate is calculated from volumetric flow rate ( $Q$ , scf/d) as follows:

$$Q_m = \frac{Q \rho_{sc}}{86,400} \quad (5)$$

Friction factor ( $f$ ) is a function of Reynolds number ( $Re$ ), and inner diameter and roughness of tubing. If  $Re$  is less than 2000 (i.e. laminar flow conditions or low flow velocities),  $f$  can be calculated as:  $f = 64/Re$ . At high velocities  $Re$  is significantly greater than 2000 (i.e. turbulent flow conditions) and  $f$  can be calculated using empirical equations such as the Colebrook-White equation (Colebrook and White, 1937) as follows:

$$\frac{1}{f^{1/2}} = -2 \log \left[ \frac{2.51}{Re f^{1/2}} + \frac{k}{3.72 d} \right] \quad (6)$$

Reynolds number ( $Re$ ) is the ratio of the inertial force to viscous or friction force;

$$Re = \frac{1488 \rho d v_m}{\mu_m} \quad (7)$$

Because  $f$  appears on both sides of eq. (6), an iterative approach was adopted to estimate  $f$ . Other empirical equations available in the technical literature such as those developed by Drew et al. (1932) for smooth pipes, and Swamee and Jain (1976) for pipes with relative roughness between  $10^{-7}$  and  $10^{-2}$ , can also be used to calculate  $f$  at turbulent flow conditions explicitly. Lastly, pressure change ( $\Delta p_i$ ) from  $p_{avg}$  and  $T_{avg}$  to another  $p_{avg}$  and  $T_{avg}$  is iteratively calculated, until it converges to a predetermined relative error ( $\epsilon = 10^{-5}$ ), using eq. (8).

$$\epsilon = \frac{\Delta p_i - \Delta p_{i-1}}{\Delta p_{i-1}} \quad (8)$$

After convergence the depth ( $h_i$ ), temperature ( $T_i$ ),  $p_{grad}$  and pressure ( $p_i$ ) for the next cell are calculated. The initial guess of  $p_{grad}$ , used to calculate  $p_i$ , for proceeding cells is estimated as:  $p_{grad} = \Delta p_{i-1} / \Delta h$ . These parameters are used to calculate  $T_{avg}$  and  $p_{avg}$ , which are also used to calculate the corresponding density, viscosity, velocity, Reynolds number, friction factor, and eventually pressure change. These calculations are repeated until convergence is achieved. This process continues until  $h_i$  is equal to  $D$  and pressure at such depth is equivalent to BHP of the well. A workflow depicting the algorithm or procedure used to calculate CO<sub>2</sub> injection BHP using modified HB model is presented in Fig. 3. Fig. 4 shows an example of density, pressure, and temperature variations from wellhead to bottom during CO<sub>2</sub> injection. Pressure and temperature increase linearly while density increases nonlinearly with depth. As a result, accurate estimates of CO<sub>2</sub> density as a function of pressure and temperature is critical in calculating wellbore pressure changes, especially at near critical conditions.

### Sensitivity analysis

#### Cell size effect.

Simulations were performed to assess the sensitivity of calculated BHP to changes in cell size (i.e. the number of cells the total well depth ( $D$ ) is broken into,  $\Delta h$ ). Values of  $\Delta h$ , as fraction of  $D$ , simulated include 1/10<sup>th</sup> (5%), 1/100<sup>th</sup> (50%), 1/200<sup>th</sup>, and 1/300<sup>th</sup> (150%) (Table 1). The case with  $\Delta h$  equal to 1/200<sup>th</sup> was considered as the baseline, which is about 32 ft for IBDP's CCS1 injection well that has a  $D$  of 6325 ft.

The results are essentially the same for the cases with  $\Delta h$  equal to 1/100<sup>th</sup>, 1/200<sup>th</sup>, and 1/300<sup>th</sup> of the  $D$ . The 1/10<sup>th</sup>  $D$  case has the fewest number of increments and has the highest friction pressure loss compared to the other cases, i.e., 5% or 1/10<sup>th</sup>  $D$  is about 630 feet. Since the other percentages (smaller increments) are all the same this indicates that 630 ft step size is too large. Therefore, the step sizes in the 1/100<sup>th</sup>, 1/200<sup>th</sup>, or 1/300<sup>th</sup>  $D$  cases are small enough to allow for accurate calculation of injection BHP (Fig. 5, top left).

#### Pipe roughness effect.

Three simulations were performed to assess the sensitivity of injection BHP to changes in pipe roughness, using relatively smooth pipe roughness as baseline. The roughness of smooth pipe reported in the technical literature is about 0.00015 inches (API 1981). Two simulations with roughness equivalent to 5% and 150% of the smooth pipe roughness were also simulated, i.e. 0.0000075 inches and 0.000225 inches, respectively. Simulation results (Fig. 5, top right) indicate that pressure change due to friction is negligible at injection rates less than 6000 Mscf/d. Results in Fig. 5 also shows that BHP is unaffected by fairly large changes in pipe roughness.

#### Friction factor and Reynolds number.

Simulations to evaluate the impact of changes in friction factor ( $f$ ) on calculated BHP were also performed. The  $f$  used as baseline, calculated using CCS1 injection data, is about 0.02. Two additional cases with friction factors equal to 5% (0.001) and 150% (0.03) of the baseline value were simulated. Simulation results suggest that pressure change due to friction loss increases with increasing friction factor. The simulation results also show pressure change due to friction loss to be negligible at injection rates less than 10,000 Mscf/d (Fig. 5, bottom). No noticeable change in calculated BHP was achieved due to large changes in Reynolds number.

### Uncertainty of the Calculated CO<sub>2</sub> injection BHP

Pressure change ( $\Delta p$ ) along the wellbore is dependent on the pressure traverse across each modeled cell of the well (i.e. eq. [3]). Calculated BHP is equivalent to the objective function ( $R$ ) with variables  $X = x_1, x_2, x_3, \dots, x_n$ , for which uncertainty will be estimated. The variables of BHP may include  $\Delta h$ ,  $\rho$ ,  $T_{wh}$ ,  $p_{wh}$ ,  $v$ ,  $f$ , etc., and is mathematically represented as follows;

$$R = f(X = x_1, x_2, x_3, \dots, x_n) \quad (9)$$

The standard deviation ( $\sigma$ ) of  $R$  or BHP can be expressed as a function of the standard deviation of its variables as follows;

$$\sigma_R = f(\sigma_{x_1}, \sigma_{x_2}, \sigma_3 \dots \sigma_{x_n}) \quad (10)$$

The uncertainty in BHP can be calculated as follows:

$$\sigma_R = \sqrt{\left(\frac{\partial R}{\partial x_1} \sigma_{x_1}\right)^2 + \left(\frac{\partial R}{\partial x_2} \sigma_{x_2}\right)^2 + \dots + \left(\frac{\partial R}{\partial x_n} \sigma_{x_n}\right)^2} \quad (11)$$

However, the BHP of the wellbore is calculated as the sum of the  $\Delta p$  of all cells from the top to bottom of the well and the wellhead pressure ( $p_{wh}$ ), i.e.,

$$BHP = p_{wh} + \sum_{h=0}^{h+n\Delta h} \frac{\left(\frac{g}{gc}\right)\rho_m + \frac{f_m \rho_m v_m^2}{64.4d}}{144} \Delta h \quad (12)$$

Thus, variables of BHP consist of the following,  $p_{wh}$ ,  $\Delta h$ ,  $\rho_m$ ,  $f_m$ , and  $v_m$ . There is some uncertainty associated with measurement of  $p_{wh}$ . However, there is no uncertainty in  $\Delta h$  because it is a fraction of the well depth and can be accurately calculated when well depth is known. The density of CO<sub>2</sub>, which is estimated from correlation of NIST data, has some uncertainty. Friction factor ( $f_m$ ) is a function of pipe roughness and Reynolds number ( $R_e$ ) and has some uncertainty. Reynolds number is also a function of density, velocity (calculated from injection rate), tubing diameter, and viscosity. As a result,  $f_m$  has some uncertainty, mostly at injection rates greater than 10,000 Mscf/d (Fig. 5) during which pressure change due to friction is significant. Generally, users familiar with the problem will separately estimate the uncertainty of the components. As a result, eq. 11 can be applied on eq. 12 to derive the uncertainty of BHP as follows;

$$\sigma_{BHP} = \sqrt{\left(\frac{\partial BHP}{\partial p_{wh}} \sigma_{p_{wh}}\right)^2 + \left(\frac{\partial BHP}{\partial \rho_m} \sigma_{\rho_m}\right)^2 + \left(\frac{\partial BHP}{\partial f_m} \sigma_{f_m}\right)^2} \quad (13)$$

As an example, eq. 13 can be applied to the input parameters and their corresponding uncertainties (Table 2) to estimate the uncertainty of calculated BHP as follows;

- 1.)  $\frac{\delta BHP}{\delta p_{wh}} \times \sigma_{p_{wh}} = 1.0 \times 22.56 = 22.56 \text{psi}$
- 2.)  $\frac{\delta BHP}{\delta \rho_m} \times \sigma_{\rho_m} = \frac{\Delta h}{144} \times 1.52 = \frac{6325}{144} \times 1.52 = 66.76$
- 3.)  $\sigma_{BHP} = \pm \left( \frac{\delta BHP}{\delta p_{wh}} \times \sigma_{p_{wh}} + \frac{\delta BHP}{\delta \rho_m} \times \sigma_{\rho_m} + \frac{\delta BHP}{\delta f_m} \times \sigma_{f_m} \right)^{1/2} = (22.56^2 + 66.76^2 + 0)^{1/2}$

Thus,  $\sigma_{BHP} = \pm 70.47 \text{psi}$

In the above example, friction pressure change is assumed negligible compared to change in hydrostatic pressure. If the calculated BHP is equivalent to 3331 psi, the calculated BHP uncertainty will be  $\pm 2.1\%$ .

### Modified HB model validation

The modified HB model was applied to injection data, recorded during implementation of the Illinois Basin-Decatur Project (IBDP) and Industrial Carbon Capture and Sequestration Project (ICCS), to predict bottom hole tubing gauge pressure (BTP) during CO<sub>2</sub> injection. The injection wells of the IBDP and ICCS are CCS1 and CCS2, respectively. About a million metric tonnes of 99% pure CO<sub>2</sub> was injected over a period of three years (i.e., from November 2011 to November 2014) via CCS1. Injection operations at the ICCS site, which is ongoing, began in May 2017 at rates greater than that of IBDP (Table 3). Both injection wells (CCS1 and CCS2) are equipped with piezoelectric gauges and flowmeters at the wellhead and tubing bottom to monitor pressure, temperature, and injection rates. Downhole gauges in both wells were mounted on top of a high temperature-high pressure Quantum MAX packer manufactured by Schlumberger. A digital temperature sensing (DTS) system consisting of a fiber optic cable that measures temperature within a thousandth degree of accuracy was installed to record temperature every 1.6 ft (0.5 m) from the surface to total depth (Table 4). Data from both wells were recorded every 30 seconds and transmitted to a centralized data collection system for analysis. Faulty outliers in the injection data were identified and removed prior to application of the modified HB model. Lastly, the accuracy of the modified HB model was assessed by comparing BTP predictions to measured field data.

Hourly averaged injection data from CCS1 and CCS2 were used to assess the accuracy of the modified HB model BTP predictions. High-level statistical analyses of the data indicate that the injection rate,  $p_{wh}$  and BHP are more dispersed (i.e. high standard deviation) than BHT and WHT (Table 4). Injection data analyses also indicate that injection rate is the most while BHT is the least dispersed data (lowest standard deviation). Thus, the accuracy of BTP calculations is highly dependent on accuracy of injection rate data, which agrees with the uncertainty analysis presented in eq. (13). Results in Table 4 also suggest that the injection data contain faulty data points; for example, the maximum injection for CCS1 and minimum WHT for CCS2 are unrealistic. As a result, faulty data points were identified and deleted from injection data.

The injection data was further reviewed to identify and remove faulty outliers in the dataset (Table 5) including but not limited to 1.) injection rates out of the specified ranges, 2.)  $p_{wh}$  greater than the specified maximum injection pressure, 3.)  $p_{wh}$  greater than BHP, and 4.) WHT less than target injection temperature (Table 3). Data points with zero injection rate represent periods in which the well was shut-in or killed during routine maintenance at the nearby ADM ethanol plant (CO<sub>2</sub> source), periodic compressor maintenance (Finley, 2014) or due to repair/replacement of faulty downhole gauges. Instances in which  $p_{wh}$  is greater than BHP were considered faulty because injection BHP is the sum of  $p_{wh}$  and hydrostatic pressure (i.e. assuming friction and acceleration pressure are negligible, Fig. 5). Data points with WHT greater than BHT were also considered faulty because temperature increases with depth. Lastly, data points with WHT less than 60 °F were removed because the injection wells were operated at WHT significantly greater than 55 °F, at which CO<sub>2</sub>-water hydrates could precipitate (Jones and McKaskle, 2014).

Fig. 6 shows histograms depicting distribution of rate and  $p_{wh}$  data for CCS1 and CCS2 injection wells. The rate and  $p_{wh}$  data distributions for CCS1 are reverse lognormal. Over 90% of the CCS1 rate and  $p_{wh}$  data are above 18000 Mscf/d and 1200 psi, respectively. On the other hand, the rate data for CCS2 are multimodally (*XXX NOTE: IS multimodally A REAL WORD??XXX*) distributed while the  $p_{wh}$  is normally distributed. However, the rate and  $p_{wh}$  data in Fig. 8 corroborate the ranges or limits specified in Table 3.

Application of the modified HB model to CCS1 and CCS2 injection data predict the measured BTP within 3% and 1% average relative error, respectively. Modeling results also suggest that hydrostatic pressure change is dominant during injection of CO<sub>2</sub> via vertical wells. Pressure changes due to friction loss and acceleration of injected CO<sub>2</sub> are of similar order of magnitude and significantly lower than changes in hydrostatic pressure (Fig. 7). Thus, calculations that assume negligible contributions from friction loss and acceleration energy terms could be used to make reasonable estimates of pressure traverse in vertical pipes or conduits.

Modeling results also show a strong positive linear correlation between modified HB model predictions and the BTP data of both CCS1 and CCS2 injection wells (Fig. 8). However, the correlation between modified HB model predictions and CCS2 well BTP data is stronger compared to CCS1 (Table 6). For example, the linear correlation coefficient ( $R^2$ ) between model predictions and BTP data is 0.81 and 0.99 for CCS1 and CCS2, respectively. Nevertheless, the modified HB model can predict measured BTP accurate enough for engineering calculations (i.e. 3-5% average relative error).

## Discussion

The original Hagedorn-Brown correlation was developed using data from a 1500 ft well with tubing from 1¼ to 2⅞ tubing. Gas and oil mixtures and viscosities from 10 –110 cp were used. Holdup or percent liquid by volume was not measured but was used to balance the losses. The flow pattern was not measured. Friction was originally from the Moody diagram with a two-phase Reynolds number. As mentioned, here the Colebrook-White equation or Jain explicit equation was used for friction factor calculation. The density and viscosity of CO<sub>2</sub> was brought in using outside studies for CO<sub>2</sub> such as NIST database (Lemmon et al. 2019) and Ouyang (2011) correlation. Use was made of the existing logic to iterate each cell for the properties and friction at the average pressure and fluid properties of each cell. Use was made of the calculations for pressure changes due to elevation (hydrostatic), friction loss, and acceleration (found to be negligible) of injected CO<sub>2</sub> in the program. The final comparative results show that pressure change due to elevation (hydrostatic) is dominant over friction loss and acceleration in vertical wells. As a result, correlation of the density of CO<sub>2</sub> from NIST database is important to be able to get calculations with only a few percent of error from the actual. It is possible that other multiphase flow industry pressure drop correlations could have been used similarly to achieve good results but use of the Hagedorn-Brown correlation modified for the injection of CO<sub>2</sub> here gave good results with a fairly simple final correlation. A model could have been completely constructed but to begin with the existing structure of the HB model was more expedient. Those needing a prediction for injection BHP should see that the method presented here is accurate as results compare to measured data. For the range of data studied here it is difficult to see what could be done to enhance the model's accuracy, unless better correlations appear for the density of CO<sub>2</sub>.

## CONCLUSION

A modified Hagedorn-Brown model, two-phase flow model, based on Hagedorn-Brown (1965) correlation with Griffith (1961) correlation modification for bubble flow and no-slip liquid holdup was developed to predict wellbore pressure changes during CO<sub>2</sub> injection. Data used as input to the model include CO<sub>2</sub> density and viscosity, surface injection rate, wellhead temperature and pressure, and bottom hole temperature. Carbon dioxide density and viscosity data from NIST database, correlated within 2 - 3% margin of error, were used to improve accuracy of model predictions. Parameter sensitivity indicate that wellbore pressure change due to hydrostatic pressure gradient is significantly greater than friction and acceleration pressure gradients during CO<sub>2</sub> injection in vertical wells.

The modified Hagedorn-Brown model predicted measured bottom hole tubing pressure data from the Illinois Basin Decatur Project and Industrial Carbon Capture and Sequestration project, two large-scale CO<sub>2</sub> storage projects, within 1-3% relative error, which is reasonably accurate for engineering calculations and validate robustness of the model in estimating wellbore pressure changes during CO<sub>2</sub> injection. Thus, the model can be used to calculate BHP from wellhead pressure corrections or predict measured bottom hole pressure when installed downhole gauges fail during CO<sub>2</sub> injection. Robustness of the modified HB model can be further validated when historical injection data from other large-scale CO<sub>2</sub> storage projects become available. An algorithm for application of the modified HB model to field data from other CO<sub>2</sub> storage projects was developed to calculate pressure traverse and bottom hole flowing pressure during injection. The model can be extended to calculate pressure changes in horizontal and inclined CO<sub>2</sub> injection wells. A relatively simple model was settled on as being accurate, but this would have not been known without this investigation.

## Nomenclature

$dp/dh$  = pressure gradient in the pipe [psi/ft]  
 $\rho$  = fluid density [lbm/ft<sup>3</sup>]  
 $\theta$  = angle of inclination of pipe from the horizontal [-]  
 $v$  = superficial fluid flow velocity [ft/s]  
 $\mu_m$  = viscosity [cp]  
 $f$  = friction factor [-]  
 $d$  = internal diameter of tubing [ft]  
 $dh$  = change in depth [ft]  
 $g$  = acceleration due to gravity [32.2 ft/s<sup>2</sup>]  
 $g_c$  = gravitational constant [32.2 lb<sub>m</sub>-ft/lb<sub>f</sub>-s<sup>2</sup>]  
 $M_t$  = total mass flow rate [lb<sub>m</sub>/d]  
 $\rho_m$  = in situ average density [lb<sub>m</sub>/ft<sup>3</sup>]  
 $v_m$  = superficial flow velocity [ft/s]  
 $Q_m$  = mass flow rate [lb/s]  
 $\rho_{sc}$  = density of CO<sub>2</sub> at standard temperature and pressure [ $\approx$ 0.115 lbm/ft<sup>3</sup>]  
 $Re$  = Reynolds number [-]  
 $k$  = roughness of duct, pipe or tube surface [ft]  
 $T$  = temperature [°F]  
BTP = Bottomhole tubing pressure [psi]  
BHP = Bottomhole pressure [psi]  
BHT = Bottomhole temperature [°F]  
 $T_{surf}$  = surface temperature [°F]  
 $p_{wh}$  = wellhead pressure [psi]  
 $q$  = injection rate [Mscf/d]  
 $\Delta h$  = cells (segments) size  
 $h_i$  = depth of current cell [ft]  
 $h_{i-1}$  = depth of previous cell [ft]  
 $p_i$  = pressure at the bottom of current cell [psi]  
 $p_{i-1}$  = pressure at the bottom of previous cell [psi]  
 $p_{grad}$  = cell pressure gradient [psi]  
 $p_{avg}$  = cell average pressure [psi]

$T_{surf}$  = wellhead temperature (WHT) [°F]  
 $T_i$  = temperature at the bottom of current cell [°F]  
 $T_{i-1}$  = temperature at the bottom of previous cell [°F]  
 $T_{avg}$  = cell average temperature [°F]

## ACKNOWLEDGMENTS

This work was supported by the U.S. Department of Energy under award number DE-FC26-05NT42588. The authors thank Damon Garner, Nick Malkewicz, Scott Frailey, ..., and Sherilyn Williams-Stroud, for constructive reviews, comments, and the data provided. We also want to thank Sallie Greenberg ensuring availability of resources required to complete this study. We also wish to acknowledge Landmark Graphics for use of their software via the University Donation Program and Schlumberger Carbon Services for donation of the Petrel E&P software platform.

## REFERENCES

- Ansari, A.M., Sylvester, N.D., Sarica, C., Shoham, O., and Brill, J.P. 1994. A comprehensive mechanistic model for upward two-phase flow in wellbores. *SPE Prod & Fac* (May 1994) 143, *Trans. AIME* **5** (297).
- API, 1981. Design and installation of offshore production platform piping systems. Third edition, API RP14E, 22, Dallas Texas.
- Brown, B.E. 1977. *The Technology of Artificial Lift Methods*. PPC Books, Tulsa, Oklahoma.
- Colebrook, C. F.; White, C. M. 1937. Experiments with Fluid Friction in Roughened Pipes. *Proc.*, Royal Society of London. Series A, Mathematical and Physical Sciences. **161** (906): 367–381.
- Fancher, G.H., and Brown, K.E. 1963. Prediction of Pressure Gradients for Multiphase Flow in Tubing. *SPE J.*, **3** (59).
- Drew, T. S., Koo, E. C. and McAdams, W. H. 1932. The friction factor in clean, round pipes. *Transactions of the American Institute of Chemical Engineers*, **28** (56).
- Finley, R.J. 2014. An overview of the Illinois Basin-Decatur Project. *Greenhouse Gases: Science and Technology* **4**. 10.1002/ghg.1433.
- Griffith, P. and Wallis, G.B. 1961. Two-phase slug flow. *Trans. ASME* 83 (Ser. C): 307-320.
- Guo, B., Lyons, W.C. and Ghalambor, A. 2007. *Petroleum Production Engineering: A Computer-Assisted Approach*. Boston: Gulf Professional Publishing (Elsevier).
- Hagedorn, A.R. 1964. *Experimental Study of Pressure Gradients Occurring During Continuous Two-Phase Flow in Small Diameter Vertical Conduits*. PhD Dissertation, The U. of Texas,
- Hagedorn, A.R. and Brown, K.E. 1965. Experimental Study of Pressure Gradients Occurring During Continuous Two-Phase Flow in Small Diameter Vertical Conduits, *J Pet Technol* **4**: 475-484.
- Hasan, A.R. and Kabir, C.S. 2002. *Fluid flow and heat transfer in wellbores*. Society of Petroleum Engineers, Richardson, Texas.
- Hovorka, S. D., Meckel, T.A., Trevino, R.H. 2013. Monitoring a large-volume injection at Cranfield, Mississippi — Project design and recommendations. *International Journal of Greenhouse Gas Control* **18**, 345–360.
- Lemmon, E.W., McLinden, M.O. and Friend, D.G. "Thermophysical Properties of Fluid Systems" in NIST Chemistry WebBook, NIST Standard Reference Database Number 69, Eds. P.J. Linstrom and W.G. Mallard, National Institute of Standards and Technology, Gaithersburg MD, 20899, <https://doi.org/10.18434/T4D303>, (retrieved October 23, 2019)
- Locke II, R., Iranmanesh, A., Wimmer, B., Kirksey, J., Malkewicz, N., and Greenberg S. 2018. Verification Well#1: How a deep monitoring well was used and adapted to meet the evolving monitoring needs and challenges at the Illinois Basin-Decatur Project. Presented at the 14<sup>th</sup> International Conference on Greenhouse Gas Control Technologies (GHGT-14), Melbourne, Australia, 21<sup>st</sup>–25<sup>th</sup> October 2018.
- Mach, J.M., Proano, E.A., and Brown, K.E. 1981. Application of Production Systems Analysis to Determine Completion Sensitivity on Gas Well Production. Presented at the Energy Resources Technology Conference and Exhibition, Houston, Texas, Jan.18-22. Paper 81-pet-13

- Ouyang L-B, 2011. New Correlations for Predicting the Density and Viscosity of Supercritical Carbon Dioxide Under Conditions Expected in Carbon Capture and Sequestration Operation. *The Open Petroleum Engineering Journal*, **4**, p13-21.
- Jones, R. A. and McKaskle, R. W. 2014. Design and operation of compression system for one million tonne CO<sub>2</sub> sequestration test. *Greenhouse Gas Sci Technol* **4**: 617-625. doi:10.1002/ghg.1438
- Swamee, P.K.; Jain, A.K. 1976. Explicit equations for pipe-flow problems. *Journal of the Hydraulics Division*. **102** (5): 657–664.
- Jarrell, P. M., Fox, C. E., Stein, M. H., and Webb, S. L. 2002. *Practical Aspects of CO<sub>2</sub> Flooding*, SPE Monograph Series, vol. 22. Society of Petroleum Engineers, Richardson, Texas.

## Conversions

SI Metric Conversion Factors	
bbl × 1.589873 E-01	= m <sup>3</sup>
ft × 3.048* E-01	= m
ft/sec <sup>2</sup> × 3.048* E-01	= m/sec <sup>2</sup>
°F (°F-32)/1.8	= °C
°F (°F+459.67)/1.8	= K
in. × 2.54	= cm
mscf × 18.854	= 1 metric tonne
lb × 4.53592 E-01	= kg
cp × 1.0 E-03	= Pa.s
lbm/ft <sup>3</sup> × 6.2428 E-02	= kg/m <sup>3</sup>
psi × 6.894757	= kPa

\*Conversion factor is exact.

### Author Biography:

**Roland T. Okwen** is a reservoir engineer with Illinois State Geological Survey a division of Prairie Research Institute at the University of Illinois at Urbana-Champaign. His research interests include reservoir engineering and machine learning. Okwen holds a BSc degree in chemistry from the University of Buea, an MSc Degree in petroleum engineering from the Technical University of Denmark, and a PhD degree in civil engineering from the University of South Florida.

**James F. Lea** is a  with Production & Lift Technology. His research interests include consulting, training, systems optimization, and software development. Lea is a Registered Professional Engineer in Texas, has nine US patents, and holds a B.S. and an M.S. in Mechanical Engineering from the University of Arkansas, and a Ph.D. in Mechanical Engineering from Southern Methodist University.

James F Lea is part owner of PLTechLLC (engineering consulting company) which offers consulting, training, system optimization and software development. Lea is a registered Professional Engineer (TX), has nine US patents, is author of 4 books, has over 100 scientific publications, and holds BS,MS (U of Arkansas) and the PhD degree from Southern Methodist University.

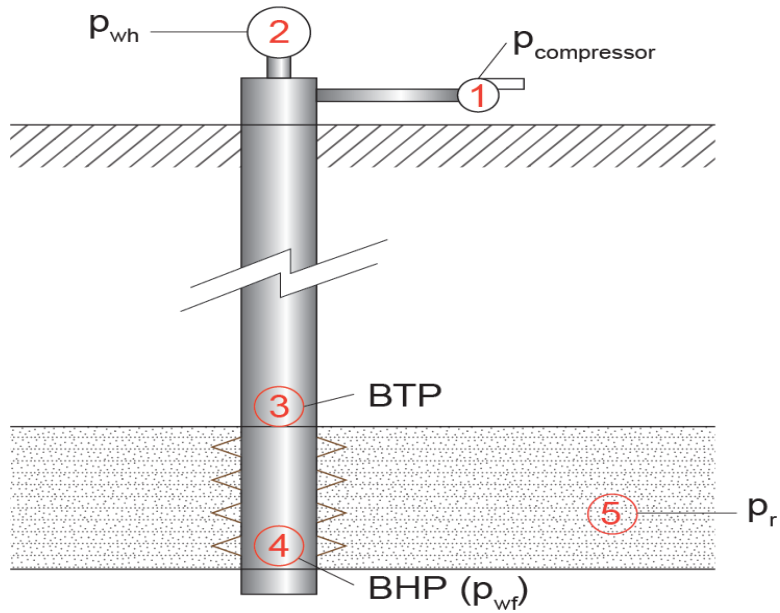


Fig. 1— Sketch showing important nodes in an injection system (adopted from Mach et al. 1981). The sketch shows BHP or pwf at the bottom of the perforated interval. However, BHP could be at the top of the reservoir interval, average across the interval or at the bottom.

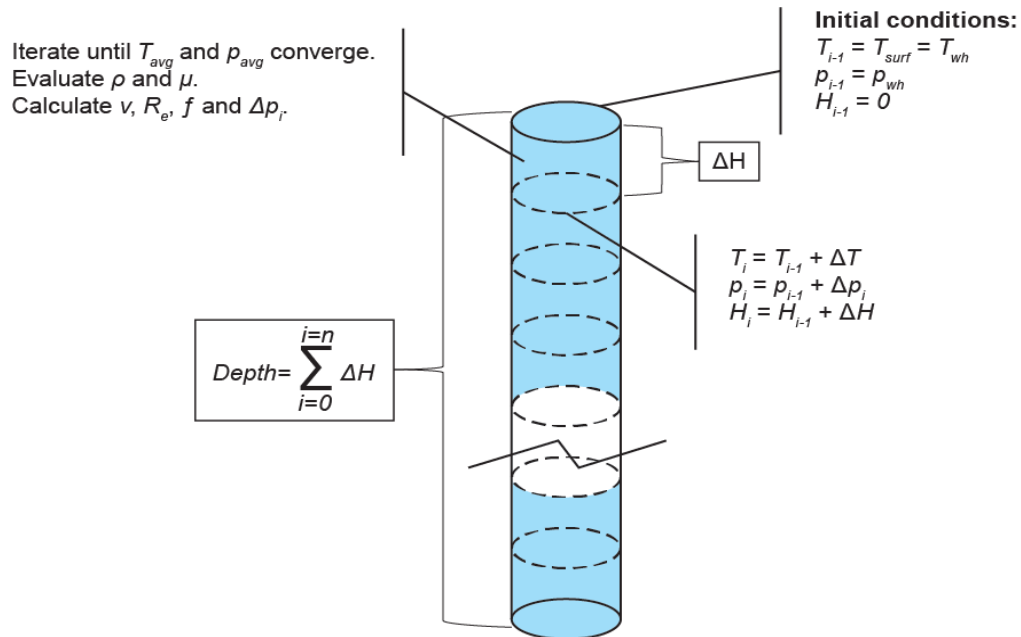


Fig. 2— Sketch illustrating how wellbore is partitioned into small cells (step-in depth).

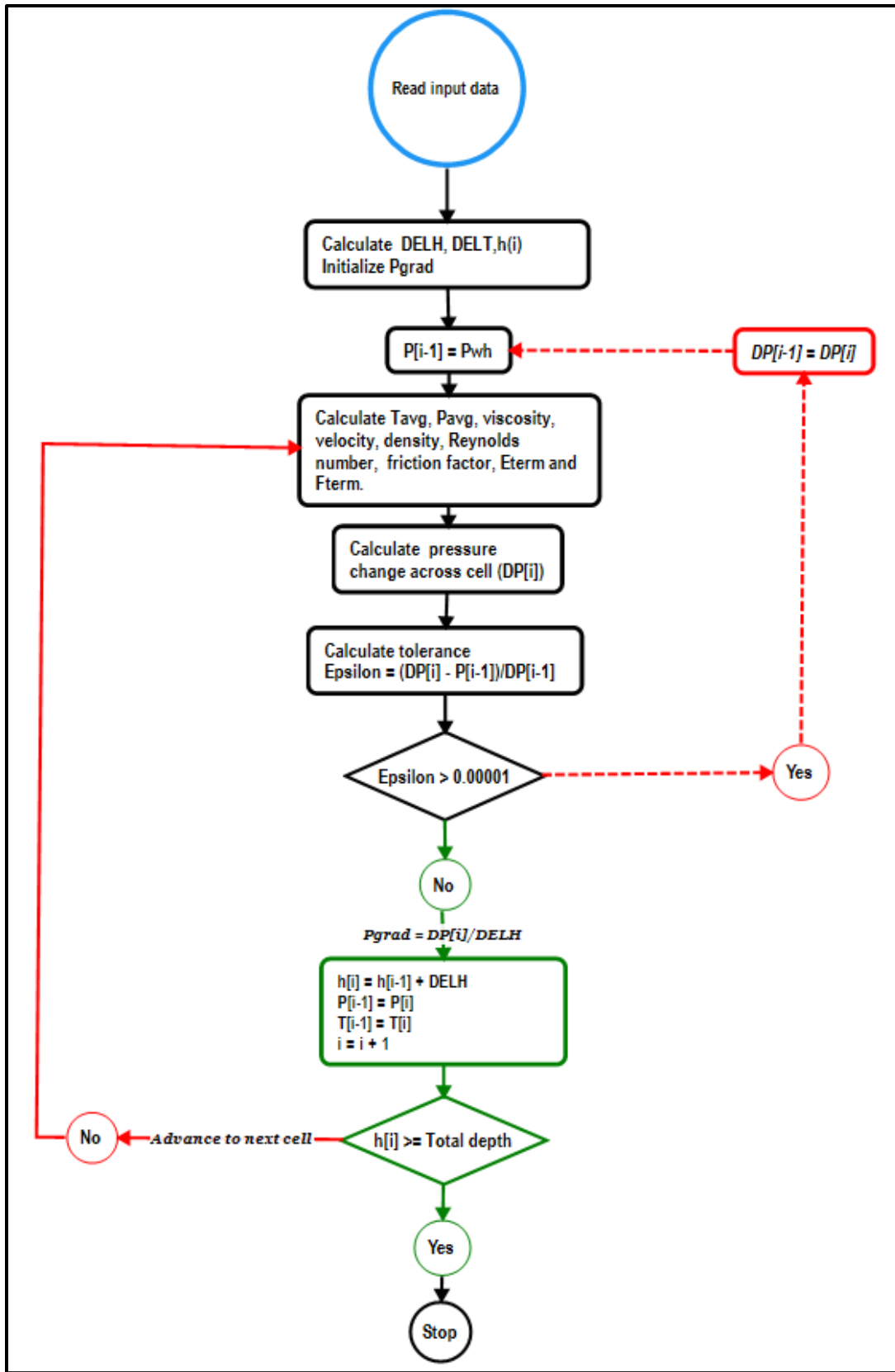


Fig. 3 — An algorithm depicting steps followed to calculate wellbore pressure transverse using the modified HB model. (Note:  $Dp = \Delta p$ ).

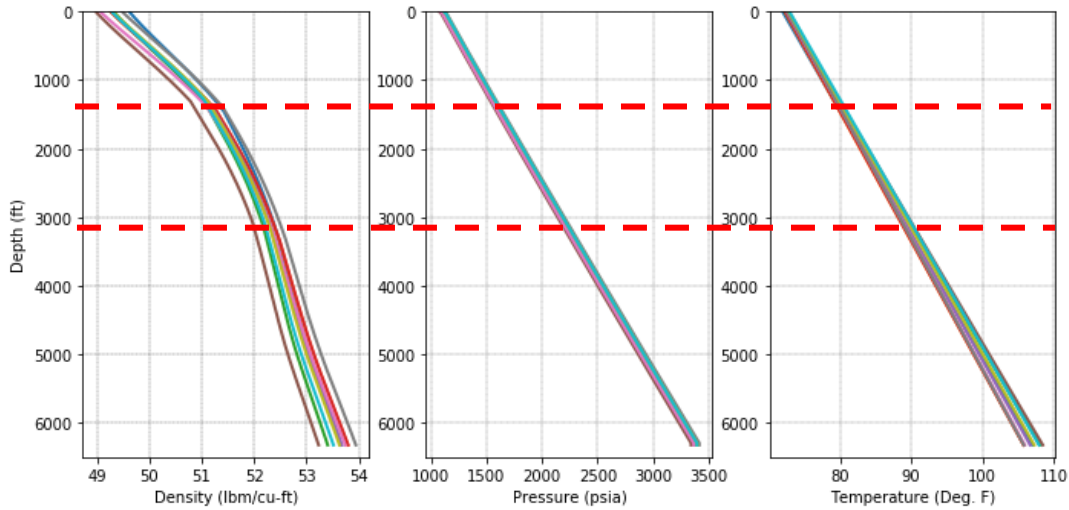


Fig. 4— Wellbore CO<sub>2</sub> density, pressure, and temperature distribution as a function of depth. The density of CO<sub>2</sub> is more sensitive to changes in temperature than pressure. Gradient of the density-depth curve changes between 80°F and 90 °F and pressures greater than the CO<sub>2</sub> critical pressure.

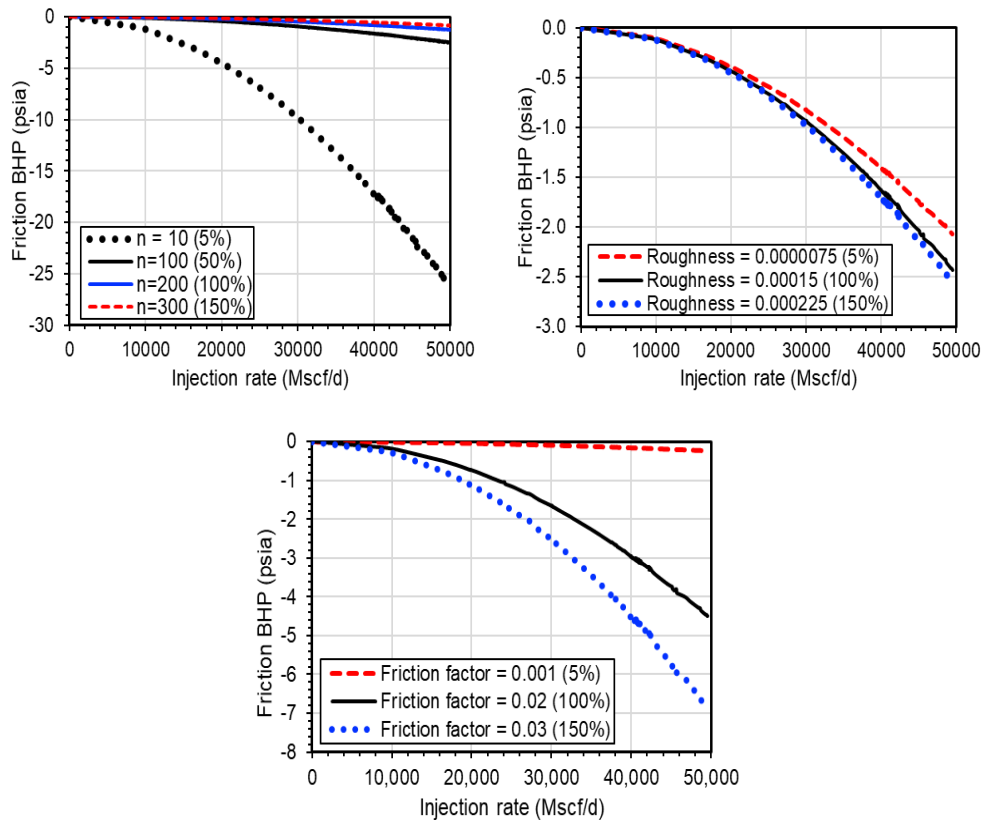


Fig. 5— Effect of changes in cell size ( $\Delta h$ , top left), pipe roughness (top right) and friction factor on calculated bottom hole friction pressure.

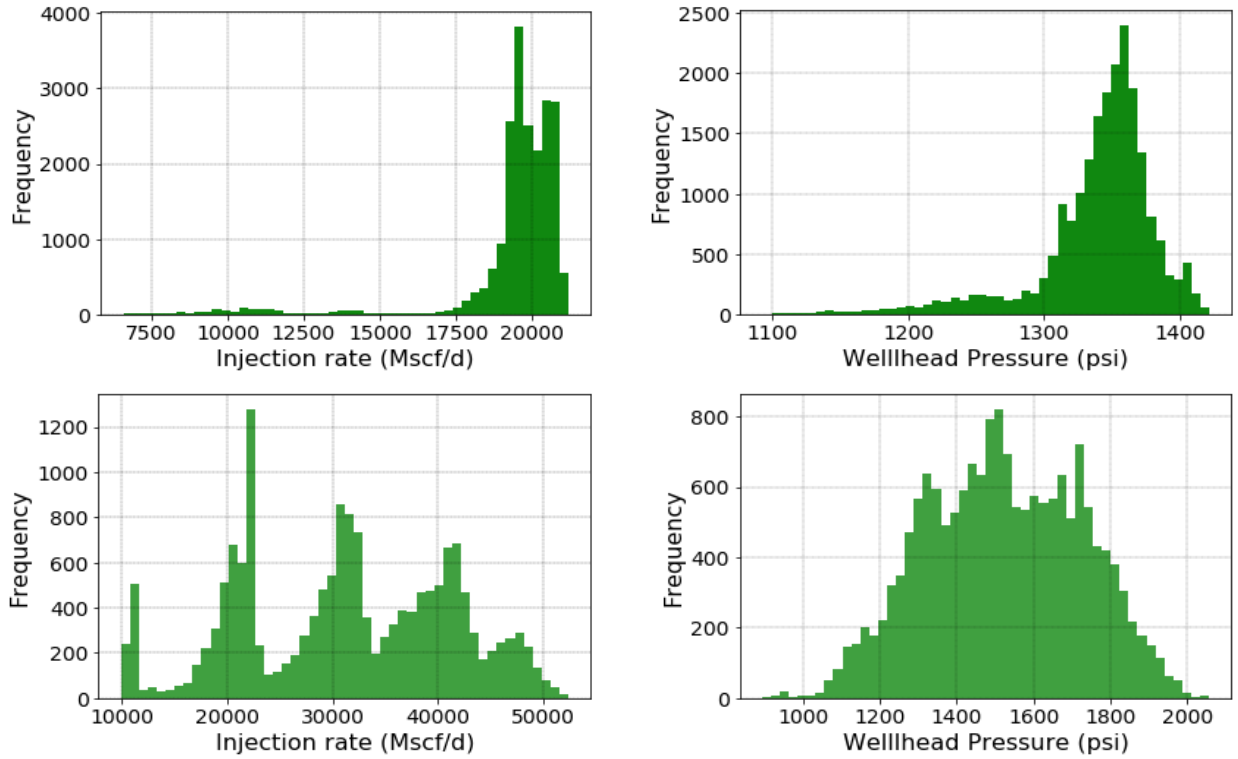


Fig. 6 — CCS1 (top) and CCS2 (bottom) surface injection rate (Left) and wellhead pressure (right) frequency distribution.

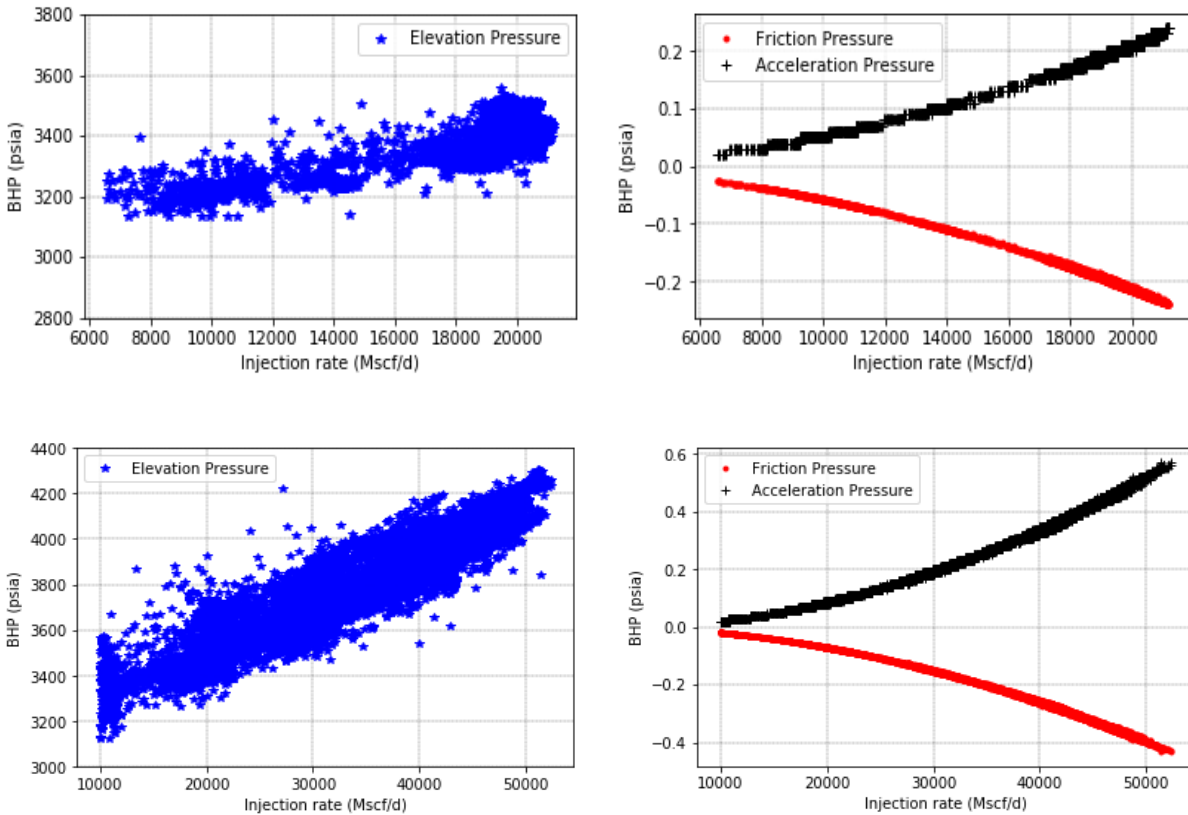


Fig. 7— Predicted hydrostatic (left) pressure and friction loss and acceleration pressures at the bottom hole gauge of CCS1 (top) and CCS2 (bottom) injection well as function of surface injection rate.

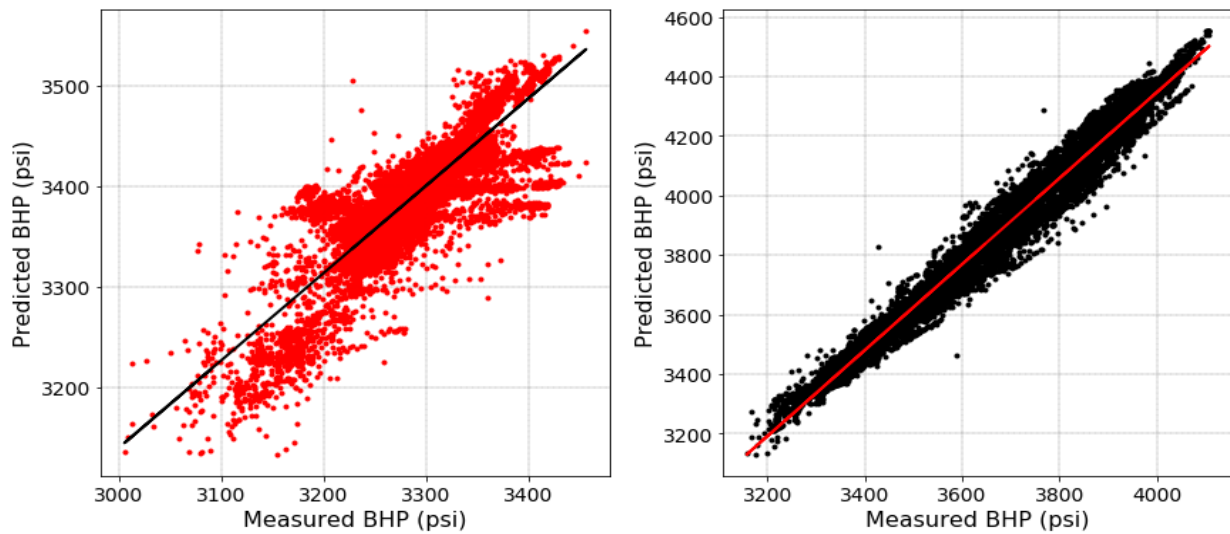


Fig. 8— Comparison modified HB model predictions and recorded hourly injection BHP from CCS1 (left) and CCS2 (right). Both Fig.s indicate that modified HB model predictions closely correlate measured BTP.

Case	Number of increments	Cell size (ft)	Percentage
Baseline (1/200 <sup>th</sup> )	200	32	100%
1/10 <sup>th</sup>	10	630	5%
1/100 <sup>th</sup>	100	63	50%
1/300 <sup>th</sup>	300	21	150%

Table 1: Simulated cell size cases. Total depth for CCS1 injection equal 6325 ft.

Parameter	Value	$\sigma$	Assumed uncertainty
Density (lbm/ft <sup>3</sup> )	76	1.52	$\pm 2\%$
Wellhead pressure (psi)	1128	22.56	$\pm 2\%$
depth (ft)	6325	0.00	$\pm 0\%$
Calculated BHP (psi)	3331	70.47	$\pm 2.1\%$

Table 2: Sample input parameters and uncertainties

	Parameter	CCS1	CCS2
	Downhole tubing gauge	Depth (ft)	6325
make		Schlumberger	Schlumberger
Model		NDPG-CA (P/N 500897)	XPQG-16-33
Type		Single (tubing)	Dual (tubing/annulus)
Other parameters	$p_{wh}$ (psig)	1000 — 1950	2284
	Q (tonnes/day)	338.4 — 1192.8	550 — 3300
	WHT (°F)	60 — 150	—
	Tubing I.D. (in)	3.96	4.89
	DTS cable <i>D</i> (ft)	6326	6211

Table 3: Well input parameters applied to modified HB model. Regulatory requirements stipulated in UIC permit of each well was used to identify and delete faulty instances.

	CCS1					CCS2				
	Wellhead		Bottom hole			Wellhead		Bottom hole		
	Q (Mscf/day)	$p_{wh}$ (psig)	WHT (°F)	BHP (psig)	BHT (°F)	Q (Mscf/day)	$p_{wh}$ (psig)	WHT (°F)	BHP (psig)	BHT (°F)
Count	29,808	22,808	22,808	22,808	22,808	17,939	17,939	17,939	17,939	17,939
mean	15,312	1,218	85	3,229	127	29,411	1,494	88	3,625	120
median	19,450	1,334	96	3,280	130	30,899	1,500	89	3,629	120

Standard deviation	31,704	639	50	176	7	12,076	226	10	220	5
minimum	0	0	0	0	0	0	536	-20	0	0
maximum	4,992,596	39,032	2,879	3,516	136	52,339	2,056	138	4,107	136
Percentiles										
25%	12,445	1,113	84	3,181	124	21,667	1,333	85	3,467	117
75%	20,166	1,360	97	3,321	131	39,256	1,669	94	3,799	123

Table 4: Description of CCS1 daily injection data.

	CCS1	CCS2
Number of instances	29808	17939
Instances with zero injection rate	6116	752
Instances with injection rates minimum limit	416	416
Instances with injection rates maximum limit	2	0
Instances with WHT < minimum limit	195	8
Instances with WHT > max limit	5	0
BHT<WHT	45	0
Instances with Pwh < 700 psi	328	0
Instances with Pwh > max limit	11	-
Instances with Pwh>BHP or BHP = 0	45	2
Tbot < 110	-	462

Table 5: Identified faulty data points deleted from the hourly average injection data. Some instances both have  $p_{wh}$  less than 700 psi and injection rates less than 338.4 tonnes/day.

	CCS1	CCS2
Number of data points	22,994	16,762
Relative error	0.004 — 8.6%	0 — 11%
Average error	3.1%	0.8%
Root mean square error*	104.7 psi	33.8 psi
Mean average error*	101.5 psi	30.9 psi
Correlation coefficient	0.867	0.997

Table 6: Modified HB model performance summary. RMSE is greater than MAE because it is more sensitive to outliers.